

Process $\eta \rightarrow \pi^0 \gamma \gamma$ in the Nambu-Jona-Lasinio model

A. E. Radzhabov* and M. K. Volkov†

Bogoliubov Laboratory of Theoretical Physics, Joint Institute for Nuclear Research, 141980 Dubna, Russia

(Received 16 October 2006; published 4 December 2006)

The decay width of the process $\eta \rightarrow \pi^0 \gamma \gamma$ is calculated in the framework of the Nambu-Jona-Lasinio model. The momentum dependence of quark loops is taken into account. Three types of diagrams are considered: quark box, scalar (a_0) and vector (ρ , ω) pole diagrams. The obtained estimations are in satisfactory agreement with recent experimental data.

DOI: [10.1103/PhysRevD.74.113001](https://doi.org/10.1103/PhysRevD.74.113001)

PACS numbers: 13.40.Hq, 11.30.Rd, 12.39.Ki, 14.40.Aq

I. INTRODUCTION

The investigations of the process $\eta \rightarrow \pi^0 \gamma \gamma$ have a long history. The experimental studies of this process began in 1966¹ [2]. The first experimental results led to a large value of the branching ratio of the process. The theoretical estimates obtained in the vector dominance model (VDM) [3], nonlinear chiral theory² [4] and lately in the chiral quark model [5–7] predicted noticeably lower value.

A real breakthrough in the investigation of this process happened in the experiment GAMS in 1981 at Protvino [8] where the large energies of the produced η -mesons dramatically suppressed the background. During a subsequent reanalysis, the value $\Gamma_{\eta \rightarrow \pi^0 \gamma \gamma} = 0.84 \pm 0.18$ eV was obtained³ [9]. Lately, the SND collaboration in the experiment VEPP-2M confirmed this value to be an upper limit 1 eV for the width of the process [1]. In 2005, the results obtained by the Crystal Ball collaboration at BNL AGS were published; these results $\Gamma_{\eta \rightarrow \pi^0 \gamma \gamma} = 0.45 \pm 0.12$ [10] were noticeably smaller than those reported by the GAMS collaboration.

From a theoretical point of view this process was investigated in many theoretical models: VDM model [3], nonlinear chiral theory [4], different quark models [5–7, 11, 12], resonance exchange models [13, 14], the chiral perturbation theory (ChPT) [15–19], and chiral unitary approach [20]. In ChPT, the main contribution comes from the terms of the order $O(p^6)$ of low energy expansion because the tree terms of the order $O(p^2)$ and $O(p^4)$ are absent and one-loop contributions of the order $O(p^4)$ are very small. The counterterms of the order $O(p^6)$ are not determined from the theory itself and should be fixed using experimental information, from the assumption of meson

saturation (vector meson exchange giving the dominant contribution) or calculated from the model (NJL, for example). In [15], the meson saturation approach was adopted, which gave $\Gamma_{\eta \rightarrow \pi^0 \gamma \gamma} = 0.18$ eV; too small, compared to the experimental value. But, keeping the momentum dependence in the vector meson propagators gives an “all-order” estimate of about 0.31 eV [15], in agreement with the old VDM prediction [3]. Taking into account the scalar and tensor meson contributions (the signs of which cannot be unambiguously determined within this approach) and the one-loop contribution at $O(p^8)$, the final estimate of [15] is $\Gamma_{\eta \rightarrow \pi^0 \gamma \gamma} = 0.42 \pm 0.20$ eV, in a satisfactory agreement with the recent Crystal Ball result. This result is confirmed in [16], where the $O(p^6)$ counterterms are calculated in the framework of the NJL model with the result 0.58 ± 0.3 eV. However, the same counterterms obtained from the NJL model by different methods lead to 0.1 eV [18] and $0.27^{+0.18}_{-0.07}$ eV [19].

The “all-order” estimations in [15] are a signal that the preservation of full momentum dependence is highly desirable. Note that in [6, 7] the simple NJL model is used without taking into account the momentum dependence of quark loops. Then, in a quark models [11, 12], the full momentum dependence of the quark box diagram is considered whereas the diagram with the intermediate scalar $a_0(980)$ is ignored. The vector sector of the model has not been taken into account as well.

In the present work, the process $\eta \rightarrow \pi^0 \gamma \gamma$ is calculated in the framework of the NJL model with scalar-pseudoscalar and vector-axial-vector sectors. The contribution of the quark box loop is considered together with the contributions of the diagrams with scalar and vector intermediate mesons (as in [6, 7]). The momentum dependence of the quark loops and pseudoscalar—axial-vector transitions are taken into account, following [21–23].

II. THE $U(3) \times U(3)$ NJL MODEL

The $U(3) \times U(3)$ NJL model with scalar-pseudoscalar and vector-axial-vector sectors is used in the present work. To solve the $U_A(1)$ problem, the six-quark t’Hooft interaction is added to the Lagrangian of the model [24, 25]

*Electronic address: aradzh@theor.jinr.ru

†Electronic address: volkov@theor.jinr.ru

¹Excellent review of theoretical and experimental works can be found in [1].²Note the similar result for the width of the order 10^{-2} eV lately obtained in ChPT for pion-loop contribution at the level $O(p^4)$.³Notice that this result is consistent with those obtained in the NJL model [6].

$$\begin{aligned} \mathcal{L} = & \bar{q}(i\hat{\partial} - m^0)q + \frac{G}{2} \sum_{i=0}^8 [(\bar{q}\lambda_i q)^2 + (\bar{q}i\gamma_5\lambda_i q)^2] \\ & + \frac{G_V}{2} \sum_{i=0}^8 [(\bar{q}\gamma_\mu\lambda_i q)^2 + (\bar{q}\gamma_5\gamma_\mu\lambda_i q)^2] \\ & - K(\det[\bar{q}(1 + \gamma_5)q] + \det[\bar{q}(1 - \gamma_5)q]), \end{aligned} \quad (1)$$

where λ_i ($i = 1, \dots, 8$) are the Gell-Mann matrices and $\lambda^0 = (\frac{2}{3})^{1/2}\mathbf{1}$, with $\mathbf{1}$ being the unit matrix; m^0 is the current quark mass matrix with diagonal elements m_u^0, m_d^0, m_s^0 ($m_u^0 \approx m_d^0$), G and G_V are the scalar-pseudoscalar and vector-axial-vector four-quark coupling constants; K is the six-quark coupling constants. The six-quark interaction can be reduced to an effective four-fermion vertex after the contraction of one of the quark pairs. The details are given in Appendix A.

Light current quarks transform to massive constituent quarks as a result of spontaneous chiral symmetry breaking. Constituent quark masses can be found from the Dyson-Schwinger equation for the quark propagators (gap equations)

$$\begin{aligned} m_u &= m_u^0 + 8m_u G I_1(m_u) + 32m_u m_s K I_1(m_u) I_1(m_s) \\ m_s &= m_s^0 + 8m_s G I_1(m_s) + 32K(m_u I_1(m_u))^2, \end{aligned} \quad (2)$$

where $I_1(m)$ is the quadratically divergent integral. The modified Pauli-Villars (PV) regularization with two subtractions with same Λ is used for the regularization of divergent integrals⁴ (see [21–23,26]). In this case the quadratically and logarithmically divergent integrals $I_1(m)$ and $I_2(m)$ have the same form as in the four-momentum cut-off scheme

$$\begin{aligned} I_1(m) &= \frac{N_c}{16\pi^2} \left[\Lambda^2 - m^2 \ln\left(\frac{\Lambda^2}{m^2} + 1\right) \right], \\ I_2(m) &= \frac{N_c}{16\pi^2} \left[\ln\left(\frac{\Lambda^2}{m^2} + 1\right) - \left(1 + \frac{m^2}{\Lambda^2}\right)^{-1} \right]. \end{aligned}$$

Moreover, the Pauli-Villars regularization is suitable for the description of the vector sector because it preserves gauge invariance.

Masses and vertex functions of the mesons can be found from the Bethe-Salpeter equation. The expression for the quark-antiquark scattering matrix is

$$\hat{T} = \mathbf{G} + \mathbf{G}\mathbf{\Pi}(p^2)\hat{T} = \frac{1}{\mathbf{G}^{-1} - \mathbf{\Pi}(p^2)}, \quad (3)$$

where \mathbf{G} and $\mathbf{\Pi}(p^2)$ are the corresponding matrices of the four-quark coupling constant and polarization loops. The particle mass can be found from the equation

⁴Any function $f(m^2)$ of mass m^2 is regularized by using the rule

$$f(m^2) \rightarrow f(m^2) - f(m^2 + \Lambda^2) + \Lambda^2 f'(m^2 + \Lambda^2).$$

$\det(\mathbf{G}^{-1} - \mathbf{\Pi}(M^2)) = 0$ and near the poles the corresponding part of the \hat{T} matrix can be expressed in the form

$$\hat{T} = \frac{\bar{V} \otimes V}{p^2 - M^2}, \quad (4)$$

where V and M are the vertex function and mass of the meson, and $\bar{V} = \gamma^0 V^\dagger \gamma^0$. Details of calculations for different channels are presented in Appendices B and C. Here we discuss only general properties.

The most simple situation takes place for the vector and the isovector scalar meson with equal quark masses (say ρ and a_0). In this case, the coupling constant and polarization operator are just numbers (not matrices). For pseudoscalar mesons, additional axial-vector components appear in the vertex function due to the pseudoscalar-axial-vector mixing (in the scalar case this transition loop is proportional to the difference of quark masses). An additional complication takes place for η and η' due to the singlet-octet mixing (or mixing of strange and nonstrange quarks due to the t'Hooft interaction). Therefore, the vertex function of this meson has four components: strange and nonstrange pseudoscalar and axial-vector.

III. FIXING MODEL PARAMETERS

The model has six parameters: the coupling constants G , G_V , K , PV cut-off Λ , and constituent quark masses m_u and m_s . We use two parametrization schemes. In the first one, the model parameters are defined using masses of the pion, kaon, ρ and η mesons and the weak pion decay constant f_π . Note that the number of input parameters is greater than the number of physical observables by one. This allows us, following [22], to take the mass of the u quark slightly larger than the half of the ρ -meson mass. As a result, we have the following set (set I) of model parameters

$$\begin{aligned} m_u &= 390 \text{ MeV}, & m_s &= 496 \text{ MeV}, \\ G &= 6.62 \text{ GeV}^{-2}, & G_V &= -11.29 \text{ GeV}^{-2}, \\ K &= 123 \text{ GeV}^{-5}, & \Lambda &= 1 \text{ GeV}. \end{aligned} \quad (5)$$

The values of the current quark masses m_u^0, m_s^0 are defined from the gap Eqs. (2) $m_u^0 = 3.9 \text{ MeV}$ and $m_s^0 = 92.3 \text{ MeV}$ ($m_u^0/m_s^0 = 23.7$).

For this set of model parameters, the two-photon decay width of the η meson $\Gamma_{\eta \rightarrow \gamma\gamma} = 0.37 \text{ KeV}$, is smaller than the experimental one: $\Gamma_{\eta \rightarrow \gamma\gamma}^{\text{exp}} = 0.510 \pm 0.026$ [27].

In the set II the model parameters are fixed in order to reproduce the two-photon decay width of the η meson instead of its mass (the η meson mass in this case $M_\eta = 530 \text{ MeV}$)

$$\begin{aligned}
m_u &= 390 \text{ MeV}, & m_s &= 506 \text{ MeV}, \\
G &= 7.65 \text{ GeV}^{-2}, & G_V &= -11.29 \text{ GeV}^{-2}, \\
K &= 77 \text{ GeV}^{-5}, & \Lambda &= 1 \text{ GeV}.
\end{aligned} \quad (6)$$

The current quark masses are $m_u^0 = 3.9 \text{ MeV}$ and $m_s^0 = 92.1 \text{ MeV}$ ($m_u^0/m_s^0 = 23.6$).

IV. DECAY $\eta \rightarrow \pi^0 \gamma \gamma$

The general form of the $\eta \rightarrow \pi^0 \gamma \gamma$ decay amplitude contains two independent tensor structures [28]

$$\begin{aligned}
A(\eta \rightarrow \pi^0 \gamma \gamma) &= T^{\mu\nu} \epsilon_\mu^1 \epsilon_\nu^2, \\
T^{\mu\nu} &= A(x_1, x_2) (q_1^\nu q_2^\mu - q_1 \cdot q_2 g^{\mu\nu}) \\
&+ B(x_1, x_2) \left[-M_\eta^2 x_1 x_2 g^{\mu\nu} - \frac{q_1 \cdot q_2}{M_\eta^2} p^\mu p^\nu \right. \\
&\left. + x_1 q_2^\mu p^\nu + x_2 p^\mu q_1^\nu \right], \quad (7)
\end{aligned}$$

where p , q_1 , q_2 are the momentum of the η meson and photons, ϵ_μ^1 and ϵ_ν^2 are the polarization vectors of the photons, and $x_i = p \cdot q_i / M_\eta^2$.

The $\eta \rightarrow \pi^0 \gamma \gamma$ decay width has the form

$$\begin{aligned}
\Gamma &= \frac{M_\eta^5}{256 \pi^2} \int_0^{(1-y)/2} dx_1 \int_{x_2^{\min}}^{x_2^{\max}} dx_2 \left\{ \left| A(x_1, x_2) \right. \right. \\
&+ \frac{1}{2} B(x_1, x_2) \left. \right|^2 [2(x_1 + x_2) + y - 1]^2 \\
&+ \frac{1}{4} |B(x_1, x_2)|^2 [4x_1 x_2 - [2(x_1 + x_2) + y - 1]]^2 \left. \right\}, \\
x_2^{\min} &= (1 - 2x_1 - y)/2, \\
x_2^{\max} &= (1 - 2x_1 - y)/2(1 - 2x_1), \\
y &= M_\pi^2 / M_\eta^2. \quad (8)
\end{aligned}$$

In the NJL model the amplitude for the $\eta \rightarrow \pi^0 \gamma \gamma$ decay process is described by three types of diagrams (see Fig. 1): the quark box and exchange of scalar (a_0) and vector (ρ , ω) resonances. Let us consider these contributions in detail.

The scalar meson exchange has the simplest form. It gives a contribution only to $A(x_1, x_2)$. This contribution consists of three parts and can be written in the form (see Appendices B and C for the definition of polarization loops and vertex functions):

$$\begin{aligned}
A(x_1, x_2) &= e^2 \frac{g_{a_0 \eta \pi} (2q_1 \cdot q_2) g_{a_0 \gamma \gamma} (2q_1 \cdot q_2)}{G_{a_0}^{-1} - \Pi_{SS}^{uu}(2q_1 \cdot q_2)}, & q_1 \cdot q_2 &= M_\eta^2 \left(x_1 + x_2 - \frac{1}{2} \right) + \frac{M_\pi^2}{2} \\
g_{a_0 \gamma \gamma} (p^2) &= \frac{1}{2\pi^2} \int_0^1 dx_1 \int_0^{1-x_1} dx_2 \frac{m_u (1 - 4x_1 x_2) \Lambda^4}{(p^2 x_1 x_2 - m_u^2 - \Lambda^2)^2 (p^2 x_1 x_2 - m_u^2)} \\
g_{a_0 \eta \pi} (p^2) &= -i 2 N_c N_f \int \frac{d^4 k}{(2\pi)^4} \text{Tr}_D \{ V_{a_0} S_u(k + q_1) V_\pi S_u(k) V_\eta S_u(k - q_2) \}. \quad (9)
\end{aligned}$$

here Tr_D is the trace over Dirac indices, index Λ in the measure of integration means PV regularization of the integral and $S_j(p) = (\hat{p} - m_j)^{-1}$.

The amplitude with the vector meson (ρ , ω) exchanges consists of two quark triangles of anomalous type (see Appendix D) and the vector meson propagator. It gives the following contributions

$$\begin{aligned}
B(x_1, x_2) &= e^2 \sum_{j=\rho, \omega} \sum_{i=1,2} \frac{g_{\eta j \gamma} (M_\eta^2, M_\eta^2 (1 - 2x_i), 0) g_{\pi j \gamma} (M_\pi^2, M_\eta^2 (1 - 2x_i), 0) M_\eta^2}{G_V^{-1} - \Pi_{VV}^{uu} (M_\eta^2 (1 - 2x_i))}, \\
A(x_1, x_2) &= -e^2 \sum_{j=\rho, \omega} \sum_{i=1,2} \frac{g_{\eta j \gamma} (M_\eta^2, M_\eta^2 (1 - 2x_i), 0) g_{\pi j \gamma} (M_\pi^2, M_\eta^2 (1 - 2x_i), 0) M_\eta^2 (1 - x_i)}{G_V^{-1} - \Pi_{VV}^{uu} (M_\eta^2 (1 - 2x_i))}. \quad (10)
\end{aligned}$$

The box diagram is of a more complicated structure. It consists of three types of boxes (plus three crossed) and contains the diagrams with pseudoscalar and axial-vector components of the π and η mesons

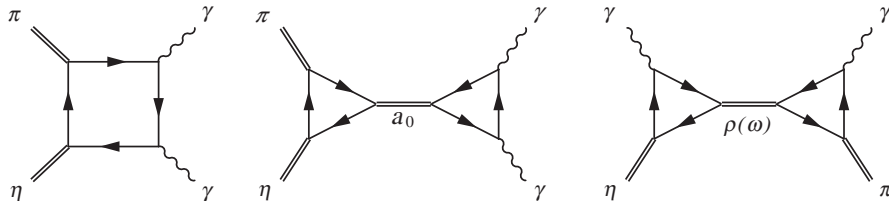


FIG. 1. Diagrams contributing to the amplitude of the process $\eta \rightarrow \pi^0 \gamma \gamma$.

$$\begin{aligned}
T_{\mu\nu} = & -ie^2 \int \frac{d^4 k}{(2\pi)^4} \text{Tr}_D(V_\eta S(k)V_\pi S(k+p-q_1-q_2)\gamma_\nu S(k+p-q_1)\gamma_\mu S(k+p) \\
& + V_\pi S(k+p)V_\eta S(k)\gamma_\nu S(k+q_2)\gamma_\mu S(k+q_1+q_2) + V_\eta S(k)\gamma_\nu S(k+q_2)V_\pi S(k+p-q_1)\gamma_\mu S(k+p) \\
& + \{q_1 \leftrightarrow q_2, \mu \leftrightarrow \nu\}).
\end{aligned} \tag{11}$$

TABLE I. $\eta \rightarrow \pi^0 \gamma \gamma$ decay width.

Contribution	set I	set II
vector mesons	0.17	0.20
scalar meson	0.03	0.12
vector + scalar mesons	0.10	0.12
box	0.28	0.35
box + vector	0.78	0.95
total	0.53	0.45

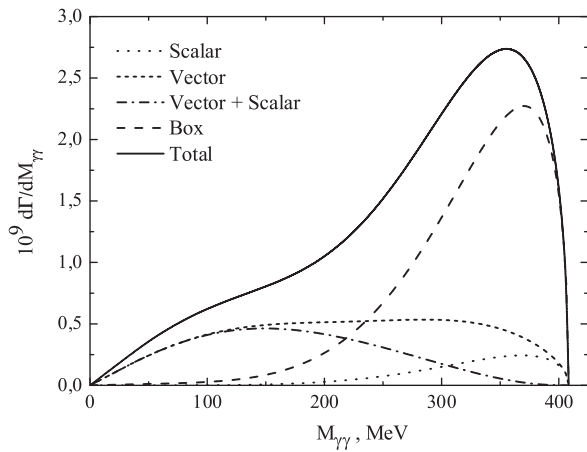


FIG. 2. Invariant mass distribution of the two-photons of the scalar meson contribution(dots), vector meson contributions(-short dash), scalar + vector mesons(dash-dot), quark box(long dash) and total(continuous line) for the set I.

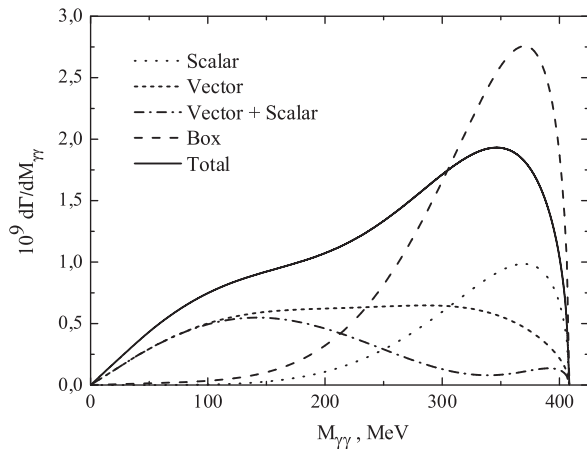


FIG. 3. Invariant mass distribution of the two-photons of the scalar meson contribution(dots), vector meson contributions(-short dash), scalar + vector mesons(dash-dot), quark box(long dash) and total(continuous line) for the set II.

We calculate these diagrams numerically. In order to check the integration procedure, we calculate all coefficients of different tensor structures and verify if they have gauge invariant form (7).

The obtained results for the decay width are given in the Table I for two sets of model parameters. The main contribution comes from the box diagram. The contribution from vector mesons has a constructive interference while the scalar a_0 contribution has a destructive one. The results are in satisfactory agreement with Crystal Ball data 0.45 ± 0.12 [10] and the present value 0.57 ± 0.21 given in PDG [27].

It is also very instructive to consider the invariant mass distribution. In Figs. 2 and 3 the invariant mass distribution of the two-photons is shown for the scalar meson contribution, vector mesons contribution, scalar + vector mesons and total. In Fig. 4, the results of our calculations of the invariant mass distribution are compared with the calculation in the chiral unitary approach [20].

V. CONCLUSIONS

Earlier calculations of the process $\eta \rightarrow \pi^0 \gamma \gamma$ in the NJL model do not include the momentum dependence of quark loops and pseudoscalar-axial-vector transitions and are in satisfactory agreement with the GAMS experiment.

Recently, the new experimental data on this decay have been obtained and the value of the decay width is almost 2 times smaller. A number of theoretical estimates is also obtained, and it seems that the momentum dependence of amplitudes is important for a correct description of this process (“all-order” estimate in ChPT).

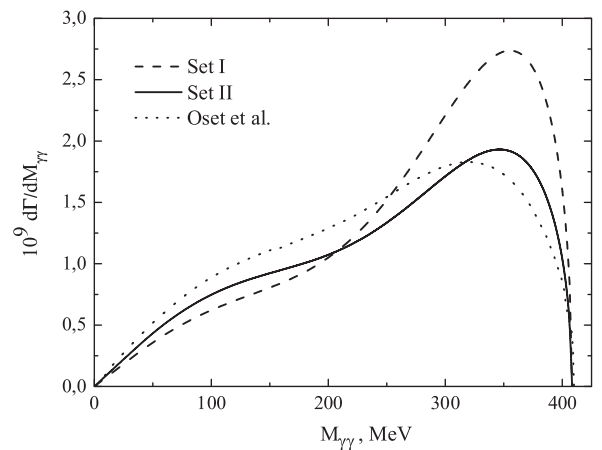


FIG. 4. Invariant mass distribution of the two-photons of the total contributions for the set I (dashes), set II (dots) together with the results of the chiral unitary approach [20].

In the present work, the contributions from quark box, scalar and vector pole diagrams are considered with the full momentum dependence. The pseudoscalar-axial-vector transitions are also taken into account.

The obtained result is consistent with recent experiments, theoretical estimates of ChPT [15,16] and the chiral unitary approach [20].

In future, we plan to consider the polarizability of pions and also decays of vector mesons $\rho(\omega) \rightarrow \eta(\pi)\pi\gamma$.

ACKNOWLEDGMENTS

The authors thank I. V. Anikin, A. E. Dorokhov, A. A. Osipov and V. L. Yudichev for useful discussions. The authors acknowledge the support of the Russian Foundation for Basic Research, under contract No. 05-02-16699.

APPENDIX A: LAGRANGIAN

Lagrangian (1) can be rewritten in the form (see [24,25])

$$\begin{aligned} \mathcal{L} = & \bar{q}(i\hat{d} - m^0)q + \frac{1}{2} \sum_{i=1}^9 [G_i^{(-)}(\bar{q}\lambda'_i q)^2 + G_i^{(+)}(\bar{q}i\gamma_5\lambda'_i q)^2] \\ & + G_{us}^{(-)}(\bar{q}\lambda_u q)(\bar{q}\lambda_s q) + G_{us}^{(+)}(\bar{q}i\gamma_5\lambda_u q)(\bar{q}i\gamma_5\lambda_s q) \\ & + \frac{G_V}{2} \sum_{i=0}^8 [(\bar{q}\gamma_\mu\lambda_i q)^2 + (\bar{q}\gamma_5\gamma_\mu\lambda_i q)^2], \end{aligned} \quad (\text{A1})$$

where

$$\begin{aligned} \lambda'_i &= \lambda_i (i = 1, \dots, 7), \\ \lambda'_8 &= \lambda_u = (\sqrt{2}\lambda_0 + \lambda_8)/\sqrt{3}, \\ \lambda'_9 &= \lambda_s = (-\lambda_0 + \sqrt{2}\lambda_8)/\sqrt{3}, \\ G_1^{(\pm)} &= G_2^{(\pm)} = G_3^{(\pm)} = G \pm 4Km_s I_1(m_s), \\ G_4^{(\pm)} &= G_5^{(\pm)} = G_6^{(\pm)} = G_7^{(\pm)} = G \pm 4Km_u I_1(m_u), \\ G_u^{(\pm)} &= G \mp 4Km_s I_1(m_s), \\ G_s^{(\pm)} &= G, \\ G_{us}^{(\pm)} &= \pm 4\sqrt{2}Km_u I_1(m_u). \end{aligned} \quad (\text{A2})$$

APPENDIX B: POLARIZATION LOOPS

Polarization loops in different channels after the PV regularization

$$e^{-izm_i m_j} \rightarrow R_{ij}(z) = e^{-izm_i m_j} [1 - (1 + iz\Lambda^2)e^{-iz\Lambda^2}] \quad (\text{B1})$$

take the form (see [22] for the expressions for the polarization loops with equal indices)

$$\begin{aligned} \Pi_{PP}^{ij}(p^2) &= \frac{N_c}{4\pi^2} \int_{-1}^1 dy \int_0^\infty \frac{dz}{z} R_{ij}(z) e^{izA} \left[-\frac{i}{z} + \frac{1}{2} p^2 (1 - y^2) - \frac{1}{2} [(m_i - m_j)^2 - y(m_i^2 - m_j^2)] \right], \\ \Pi_{SS}^{ij}(p^2) &= \Pi_{PP}^{ij}(p^2) - 2m_i m_j \frac{N_c}{4\pi^2} \int_{-1}^1 dy \int_0^\infty \frac{dz}{z} R_{ij}(z) e^{izA}, \\ \Pi_{VV}^{ij,\mu\nu}(p^2) &= \left(g^{\mu\nu} - \frac{p^\mu p^\nu}{p^2} \right) \Pi_{VV}^{ij}(p^2) + \frac{p^\mu p^\nu}{p^2} \Pi_{VV}^{ij,L}(p^2), \\ \Pi_{VV}^{ij,L}(p^2) &= \frac{N_c}{8\pi^2} \int_{-1}^1 dy \int_0^\infty \frac{dz}{z} R_{ij}(z) e^{izA} [(m_i - m_j)^2 - y(m_i^2 - m_j^2)], \\ \Pi_{VV}^{ij}(p^2) &= \Pi_{VV}^{ij,L}(p^2) - p^2 \frac{N_c}{8\pi^2} \int_{-1}^1 dy (1 - y^2) \int_0^\infty \frac{dz}{z} R_{ij}(z) e^{izA}, \\ \Pi_{AA}^{ij,\mu\nu}(p^2) &= \left(g^{\mu\nu} - \frac{p^\mu p^\nu}{p^2} \right) \Pi_{AA}^{ij,T}(p^2) + \frac{p^\mu p^\nu}{p^2} \Pi_{AA}^{ij}(p^2), \\ \Pi_{AA}^{ij,T}(p^2) &= \Pi_{VV}^{ij}(p^2) + 2m_i m_j \frac{N_c}{4\pi^2} \int_{-1}^1 dy \int_0^\infty \frac{dz}{z} R_{ij}(z) e^{izA}, \\ \Pi_{AA}^{ij}(p^2) &= \Pi_{VV}^{ij,L}(p^2) + 2m_i m_j \frac{N_c}{4\pi^2} \int_{-1}^1 dy \int_0^\infty \frac{dz}{z} R_{ij}(z) e^{izA}, \\ \Pi_{PA}^{ij,\mu}(p^2) &= \frac{p^\mu}{\sqrt{p^2}} \Pi_{PA}^{ij}(p^2) = p^\mu i(m_i + m_j) \frac{N_c}{8\pi^2} \int_{-1}^1 dy \int_0^\infty \frac{dz}{z} R_{ij}(z) e^{izA}, \\ \Pi_{AP}^{ij,\mu}(p^2) &= \frac{p^\mu}{\sqrt{p^2}} \Pi_{AP}^{ij}(p^2) = -p^\mu i(m_i + m_j) \frac{N_c}{8\pi^2} \int_{-1}^1 dy \int_0^\infty \frac{dz}{z} R_{ij}(z) e^{izA}, \\ A &= \frac{p^2}{4} (1 - y^2) - \frac{1}{2} [(m_i - m_j)^2 - y(m_i^2 - m_j^2)]. \end{aligned} \quad (\text{B2})$$

APPENDIX C: VERTEX FUNCTIONS

The most simple form have the vertex functions for the vector ρ and the isovector scalar meson a_0 , namely ⁵:

$$V_{a_0} = g_{a_0} \mathbf{I} a_0, \quad V_\rho = g_\rho \gamma_\mu \rho^\mu. \quad (\text{C1})$$

The matrices \mathbf{G} and $\mathbf{\Pi}$ for a_0 and ρ mesons have the form

$$\begin{aligned} \mathbf{G}_{a_0} &= G_1^{(-)}, & \mathbf{\Pi}_{a_0}(p^2) &= \Pi_{SS}^{uu}(p^2), \\ \mathbf{G}_\rho &= G_V, & \mathbf{\Pi}_\rho(p^2) &= \Pi_{VV}^{uu}(p^2) \end{aligned} \quad (\text{C2})$$

For the pion and kaon, additional axial-vector components appear in the vertex function due to pseudoscalar-axial-vector mixing

$$V_\pi = g_\pi i \gamma_5 (1 + \Delta_\pi \hat{p}) \pi, \quad V_K = g_K i \gamma_5 (1 + \Delta_K \hat{p}) K \quad (\text{C3})$$

Here \mathbf{G} and $\mathbf{\Pi}$ are

$$\begin{aligned} \mathbf{G}_\pi &= \begin{pmatrix} G_1^{(+)} & 0 \\ 0 & G_V \end{pmatrix}, \\ \mathbf{\Pi}_\pi(p^2) &= \begin{pmatrix} \Pi_{PP}^{uu}(p^2) & \Pi_{PA}^{uu}(p^2) \\ \Pi_{AP}^{uu}(p^2) & \Pi_{AA}^{uu}(p^2) \end{pmatrix}, \\ \mathbf{G}_K &= \begin{pmatrix} G_4^{(+)} & 0 \\ 0 & G_V \end{pmatrix}, \\ \mathbf{\Pi}_K(p^2) &= \begin{pmatrix} \Pi_{PP}^{us}(p^2) & \Pi_{PA}^{us}(p^2) \\ \Pi_{AP}^{us}(p^2) & \Pi_{AA}^{us}(p^2) \end{pmatrix}. \end{aligned} \quad (\text{C4})$$

Therefore, the vertex function of the η meson have four components: strange and nonstrange pseudoscalar and axial-vector

$$\begin{aligned} V_\eta &= g_{\eta_u} i \gamma_5 (1 + \Delta_{\eta_u} \hat{p}) \eta_u + g_{\eta_s} i \gamma_5 (1 + \Delta_{\eta_s} \hat{p}) \eta_s \\ &= g_\eta i \gamma_5 (\cos \Theta_\eta \eta_u - \sin \Theta_\eta \eta_s \\ &\quad + \Delta_\eta \hat{p} (\cos \tilde{\Theta}_\eta \eta_u - \sin \tilde{\Theta}_\eta \eta_s)), \end{aligned} \quad (\text{C5})$$

$$I_j(M_P^2, q_1^2, q_2^2) = \frac{1}{2\pi^2} \int_0^1 dx_1 \int_0^{1-x_1} dx_2 \frac{m_j}{m_j^2 - x_1(1-x_1-x_2)q_1^2 - x_2(1-x_1-x_2)q_2^2 - x_1x_2M_P^2}. \quad (\text{D3})$$

The amplitudes for the processes $\rho(\omega) \rightarrow \eta(\pi)\gamma$ have the form

$$A(PV\gamma) = g_\rho e g_{PV\gamma}(M_P^2, q_1^2, q_2^2) \epsilon_{\mu\nu\alpha\beta} \epsilon_1^\mu \epsilon_2^\nu q_1^\alpha q_2^\beta, \quad (\text{D4})$$

here q_1 and ϵ_μ^1 are the momentum and the polarization

⁵We suppress flavor indices.

where Θ_η and $\tilde{\Theta}_\eta$ are the mixing angles for pseudoscalar and axial-vector components. The matrices \mathbf{G} and $\mathbf{\Pi}(p^2)$ are four-by-four matrices

$$\begin{aligned} \mathbf{G} &= \begin{pmatrix} \mathbf{G}^{(+)} & 0 \\ 0 & \mathbf{G}_V \end{pmatrix}, & \mathbf{G}^{(+)} &= \begin{pmatrix} G_u^{(+)} & G_{us}^{(+)} \\ G_s^{(+)} & G_s^{(+)} \end{pmatrix}, \\ \mathbf{G}_V &= \text{diag}\{G_V, G_V\} \\ \mathbf{\Pi}(p^2) &= \begin{pmatrix} \mathbf{\Pi}_{PP}(p^2) & \mathbf{\Pi}_{PA}(p^2) \\ \mathbf{\Pi}_{AP}(p^2) & \mathbf{\Pi}_{AA}(p^2) \end{pmatrix}, \\ \mathbf{\Pi}_{ij}(p^2) &= \text{diag}\{\Pi_{ij}^{uu}(p^2), \Pi_{ij}^{ss}(p^2)\}, \quad i, j = P, A \end{aligned} \quad (\text{C6})$$

APPENDIX D: AMPLITUDES $\eta \rightarrow \gamma\gamma$, $\rho \rightarrow \eta(\pi)\gamma$

The amplitude for the two-photon decay width of the pseudoscalar meson has the form

$$A(P \rightarrow \gamma\gamma) = e^2 g_{P\gamma\gamma}(M_P^2, q_1^2, q_2^2) \epsilon_{\mu\nu\alpha\beta} \epsilon_1^\mu \epsilon_2^\nu q_1^\alpha q_2^\beta, \quad (\text{D1})$$

where q_1, q_2 are the momentum of photons and $\epsilon_\mu^1, \epsilon_\nu^2$ are the polarization vectors of the photons,

$$\begin{aligned} g_{\pi\gamma\gamma}(M_\pi^2, q_1^2, q_2^2) &= I_u(M_\pi^2, q_1^2, q_2^2) g_\pi, \\ g_{\eta\gamma\gamma}(M_\eta^2, q_1^2, q_2^2) &= \frac{5}{3} I_u(M_\eta^2, q_1^2, q_2^2) g_{\eta_u} \\ &\quad - \frac{\sqrt{2}}{3} I_s(M_\eta^2, q_1^2, q_2^2) g_{\eta_s}. \end{aligned} \quad (\text{D2})$$

The loop integrals $I_j(M_P^2)$ are given by

vector of $\rho(\omega)$ meson.

$$\begin{aligned} g_{\pi\rho\gamma}(M_\pi^2, q_1^2, q_2^2) &= I_u(M_\pi^2, q_1^2, q_2^2) g_\pi, \\ g_{\eta\rho\gamma}(M_\eta^2, q_1^2, q_2^2) &= 3I_u(M_\eta^2, q_1^2, q_2^2) g_{\eta_u}, \\ g_{\pi\omega\gamma}(M_\pi^2, q_1^2, q_2^2) &= 3I_u(M_\pi^2, q_1^2, q_2^2) g_\pi, \\ g_{\eta\omega\gamma}(M_\eta^2, q_1^2, q_2^2) &= I_u(M_\eta^2, q_1^2, q_2^2) g_{\eta_u}. \end{aligned} \quad (\text{D5})$$

- [1] M. N. Achasov *et al.*, Nucl. Phys. **B600**, 3 (2001).
- [2] G. D. Giugno *et al.*, Phys. Rev. Lett. **16**, 767 (1966).
- [3] G. Oppo and S. Oneda, Phys. Rev. **160**, 1397 (1967).
- [4] D. Ebert and M. K. Volkov, Sov. J. Nucl. Phys. **30**, 736 (1979).
- [5] A. N. Ivanov and N. I. Troitskaya, Yad. Fiz. **36**, 494 (1982).
- [6] D. V. Kreopalov and M. K. Volkov, Sov. J. Nucl. Phys. **37**, 770 (1983).
- [7] M. K. Volkov, Sov. J. Part. Nucl. **17**, 186 (1986).
- [8] F. Binon *et al.* (Serpukhov-Brussels-Annecy(LAPP)), Nuovo Cim. Lett. **32**, 45 (1981).
- [9] D. Alde *et al.* (Serpukhov-Brussels-Annecy(LAPP)), Z. Phys. C **25**, 225 (1984).
- [10] S. Prakhov *et al.*, Phys. Rev. C **72**, 025201 (2005).
- [11] J. N. Ng and D. J. Peters, Phys. Rev. D **47**, 4939 (1993).
- [12] Y. Nemoto, M. Oka, and M. Takizawa, Phys. Rev. D **54**, 6777 (1996).
- [13] P. Ko, Phys. Rev. D **47**, 3933 (1993).
- [14] J. N. Ng and D. J. Peters, Phys. Rev. D **46**, 5034 (1992).
- [15] L. Ametller, J. Bijnens, A. Bramon, and F. Cornet, Phys. Lett. B **276**, 185 (1992).
- [16] S. Bellucci and C. Bruno, Nucl. Phys. **B452**, 626 (1995).
- [17] P. Ko, Phys. Lett. B **349**, 555 (1995).
- [18] A. A. Bel'kov, A. V. Lanyov, and S. Scherer, J. Phys. G **22**, 1383 (1996).
- [19] J. Bijnens, A. Fayyazuddin, and J. Prades, Phys. Lett. B **379**, 209 (1996).
- [20] E. Oset, J. R. Pelaez, and L. Roca, Phys. Rev. D **67**, 073013 (2003).
- [21] V. Bernard, A. A. Osipov, and U. G. Meissner, Phys. Lett. B **285**, 119 (1992).
- [22] V. Bernard *et al.*, Ann. Phys. (N.Y.) **249**, 499 (1996).
- [23] B. Bajc *et al.*, Nucl. Phys. A **604**, 406 (1996).
- [24] S. P. Klevansky, Rev. Mod. Phys. **64**, 649 (1992).
- [25] S. Klimt, M. Lutz, U. Vogl, and W. Weise, Nucl. Phys. A **516**, 429 (1990).
- [26] C. Schuren, E. Ruiz Arriola, and K. Goeke, Nucl. Phys. A **547**, 612 (1992).
- [27] W.-M. Yao, *et al.*, J. Phys. G **33**, 1 (2006); <http://pdg.lbl.gov>.
- [28] G. Ecker, A. Pich, and E. de Rafael, Nucl. Phys. **B303**, 665 (1988).